Supporting Information

Enzyme-Driven Biodegradation of Ti_3C_2 MXene: Unveiling Peroxidase-Mediated Pathways and Enhanced Bioaccumulation Risks in Aquatic Systems

Weibiao Ye[1], Wenhao Lao[1], Lan Wu[1], Dong-Xing Guan[2], Chao Zhang[2], Yiping Feng[1*], and Liang Mao[3*]

[1]*Guangdong Key Laboratory of Environmental Catalysis and Health Risk Control, Guangzhou Key Laboratory Environmental Catalysis and Pollution Control, School of Environmental Science and Engineering, Institute of Environmental Health and Pollution Control, Guangdong University of Technology, Guangzhou 510006, China*

[2]*Zhejiang Provincial Key Laboratory of Agricultural Resources and Environment, Institute of Soil and Water Resources and Environmental Science, College of Environmental and Resource Sciences, Zhejiang University, Hangzhou 310058, China*

[3]*State Key Laboratory of Pollution Control and Resource Reuse, School of the Environment, Nanjing University, Nanjing 210023, China*

* Corresponding author: Yiping Feng, E-mail: ypfeng@gdut.edu.cn; Liang Mao, E-mail: lmao@nju.edu.cn

This file contains one supplementary 6 texts (Text S1-S6), 16 figures (Figure S1-S16) and 1 table (Table S1).

Text S1. Characterization of Ti_3C_2

The morphology of Ti_3C_2 MXene was observed by SEM, as shown in **Figure S1a.** An ultrathin, two-dimensional nanosheet structure of Ti_3C_2 MXene was observed. AFM observations indicated that the Ti_3C_2 MXene maintained its nanosheet morphology, with an average lateral size of approximately 500 nm and a thickness of 3 – 5 nm, suggesting the presence of about three layers (**Figure 1b**).[1] The crystal structure of the Ti_3C_2 nanosheet was determined by XRD characterization, as shown in **Figure S1c**. The characteristic (002) peak of pristine Ti_3C_2 nanosheets at $2\theta = 9.1°$, along with other peaks at 19.2°, 39.0°, 41.9°, and 60.8°, were assigned to Ti_3C_2 MXene (PDF# 52-0875).[2, 3] FT-IR analysis further examined surface functional groups on Ti_3C_2 MXene (**Figure S1d**). The presence of hydroxyl groups on the Ti_3C_2 surface was confirmed by absorption peaks at 3436 and 1634 cm^{-1}, attributed to absorbed external water and hydrogen-bonded OH, respectively.[4] The peaks at 621 cm^{-1} and 465 cm^{-1} in the Ti_3C_2 sample were assigned to the deformation vibration of Ti–O and Ti–C bonds,[5, 6] respectively. The Ti–O bond vibration at 621 cm^{-1} further corroborated the presence of oxygen-containing groups on the Ti_3C_2 surface.

XPS analysis was performed to examine the elemental compositions and molecular structures of the Ti_3C_2 MXene samples. **Figure S1e** shows the XPS survey spectrum of the pristine Ti_3C_2 MXene samples, revealing the presence of C1s, O1s, F1s, and Ti 2p peaks, indicating the presence of Ti_3C_2 along with the −F group introduced by the HF aqueous solution.[2] High-resolution XPS spectra of the C1s, O1s, and Ti 2p were analyzed to examine the chemical bonds in Ti_3C_2 MXene. In the C1s spectrum of Ti_3C_2 MXene (**Figure S1f**), three peaks at 281.6, 284.9, and 288.7 eV correspond to C–Ti, C–C, and C–O bonds, respectively. The high-resolution spectrum of Ti 2p (**Figure S1g**)in Ti_3C_2 MXene revealed six peaks: 460.7 eV (Ti–C 2p1/2) and 454.7 eV (Ti–C 2p3/2) representing Ti–C bonds, and 456.1, 458.8, 461.6, and 464.6 eV corresponding to Ti^{2+} (2p1/2), Ti^{4+} (2p3/2), Ti^{2+} (2p1/2), and Ti^{4+} (2p3/2) bonds,[7, 8] respectively. A small amount of TiO_2 in Ti_3C_2 possibly originated from reactions during HF treatment.[7]

The high-resolution spectrum of O1s (**Figure S1h**) indicated a small proportion of TiO_2 present on Ti_3C_2 MXene.

Text S2. Enzyme Activity Assay

HRP activity was quantified using colorimetric assay in which 2, 2'-azinobis (3-ethyl benzthiazoline-6-sulfonic acid (ABTS) is oxidized by the enzyme in a 10mM phosphate buffer (pH=6),[9-11] with continuous monitoring of absorbance at 420 nm over time. One unit of HRP activity is defined as the amount of enzyme required to mediate oxidation of 1 μmol of ATBS per min.

Text S3. Michaelis–Menten Kinetics Study

The reactions for Michaelis-Menten kinetics study were performed in 10-mL glass test tubes at room temperature. The reaction solutions initially contained various concentrations of Ti_3C_2 MXene and a consistent dosage of HRP at 0.8 U mL^{-1}. 100 μM H_2O_2 was used. The reaction solution was then mixed for 180 s using a miniature whirlpool mixture apparatus during HRP catalysis, after which 2 mL of acetonitrile was added to stop the reaction. Each initial Ti_3C_2 MXene concentration was tested in triplicate.

The parameters K_M and V_{max} of the Michaelis–Menten reaction kinetics were estimated using the initial reaction rate method. The initial reaction rate (V_0) was calculated based on the formula $V_0= (S_0-S_t)/\Delta t$ by measuring the substrate concentration in both the blank (S_0) and reaction tubes (S_t). The reaction time, Δt, was determined in preliminary tests to capture the pseudo-first-order rate behavior of the enzymatic reactions and ensure reproducible handling of the reactors. The obtained initial rate data were then fitted to the Michaelis-Menten equation $V_0 = V_{max}\times S_0 /(S_0+K_M)$ to determine the maximum rate of enzymatic reaction Vmax and the substrate's Michaelis constant (K_M). Generally, the enzyme activity ([E]) can be assumed to be the same as its initial activity ([E_0]) because the reaction time is very short (180 s). Michaelis–Menten constants were obtained by curve fitting the plot of

reaction rate versus substrate concentrations to the Michaelis-Menten equation with Sigma Plot 12.5 software (SPSS Inc., Chicago, IL).

Text S4. Ultra-Performance Liquid Chromatography-Tandem Mass Spectrometry (LC-MS/MS) Analysis

The LC–MS/MS analysis was performed a Thermo Scientific Ultimate 3000 liquid phase system equipped with Q Exactive Orbitrap and an electrospray ionization source. A volume of 5 μL sample was injected into a Hypersil Gold C18 column (100 × 2.1 mm, 1.9 μm, Thermo Scientific) at 40 °C. The flow rate was set to 250 μL/min using 0.1% formic acid and methanol (v/v = 20/80) as the eluent. The gradient program was performed as follows: 0–2 min, 98-80% A; 2–10 min, 80-5% A; 10-16 min, 5%A; and 16.1–20 min, 98% A.

Both positive and negative electrospray ionization were employed to obtain MS signals of analytes, with spray voltages of +3.5 kV and -2.5 kV, respectively. The sheath gas flow rate, aux gas flow rate, and sweep gas flow rate were set to 40, 10, and 0 mL/min, respectively. Capillary temperature and aux gas heater temperature were set to 320°C and 350°C, respectively. The instrument automatically switched between the positive and negative ion scanning modes and the scan mode was chosen as full MS scan-dd MS2 and acquired first MS signals at 70,000 FWHM and targeted MS/MS scan was set at a resolution of 175,00 FWHM with a isolation width of 0.4 m/z. Meanwhile, the m/z scan range was 50-750. Instrument control and data acquisition were performed using an Xcalibur workstation (Thermo Fisher Scientific). Data analysis was conducted using Compound Discoverer 3.2 (Thermo Scientific), and the mzCloud database (Thermo Scientific, http://www.mzcloud.org).

Text S5. *Daphnia* Exposure Experiments

The exposure concentrations of Ti_3C_2 MXene were set at 0, 0.1, 1.0, 2.0, 5.0, 10.0, 20.0, 50.0, and 100 mg L^{-1}, prepared in fresh artificial freshwater (AF) ($CaCl_2 \cdot 2H_2O$, 58.8 mg L^{-1}; $MgSO_4 \cdot 2H_2O$, 24.7 mg L^{-1}; $NaHCO_3$, 13.0 mg L^{-1}; KCl, 1.2 mg L^{-1}; hardness

$[Ca^{2+}] + [Mg^{2+}] = 0.5$ mM).[12, 13] No feeding occurred during the test. Three parallel groups were included per concentration, and the mortality of *Daphnia* was observed and recorded after 24, 48, 72, and 96 h.[14, 15]

Accumulation of Ti_3C_2 MXene by *Daphnia*, before and after biodegradation, was conducted using the method employed in our earlier study.[12] Briefly, a Ti_3C_2 MXene stock solution (5 mg mL^{-1}) was prepared using sonication and diluted in fresh AF to yield an exposure concentration of approximately 1.0 mg L^{-1} for uptake experiments. A total of 200 organisms were added to each glass beaker containing 1 L of artificial freshwater with Ti_3C_2 MXene. The control group contained the same amount of *Daphnia* in artificial freshwater without Ti_3C_2 MXene. Three replicates were used for each treatment. There was no feeding during the uptake period.

Fifteen *Daphnia* specimens from each glass beaker were sampled after 10 minutes, 0.5, 1, 3, 8, 12, 24, and 48 h of exposure. The sampled *Daphnia* specimens were placed in clean water and pipetted vigorously to remove Ti_3C_2 MXene particles attached to their carapaces. The accumulation of Ti_3C_2 MXene by *Daphnia* was directly observed using a microscope (Zeiss, Germany). The *Daphnia* specimens were then freeze-dried in a freeze dryer (Boyikang, Beijing, China) and weighed by using a Mettler Toledo microbalance. The dried *Daphnia* specimens were digested with 1.0 mL HNO_3 and H_2O_2 using a microwave digestion system (CEM MARS-6) and finally reconstituted with 2% HNO_3. Titanium concentrations were determined by inductively coupled plasma optical emission spectrometry (ICP-OES, iCAP Pro X, Thermo Fisher Scientific, USA).

Following the uptake experiments, *Daphnia* specimens in each beaker were rinsed with clean artificial freshwater and subsequently transferred to fresh beakers filled with clean artificial freshwater for depuration trials. Sampling time points of depuration were 3, 5, 10, and 24 h. Then the artificial freshwater was supplemented with *Saccharomyces cerevisiae* yeast at a concentration of 1.0×10^8 cells L^{-1}. Additional depuration samples were taken at 2.5, 5, 7, and 24 h. Sample preparation followed the same procedure as the uptake experiments. The concentration of Ti_3C_2 MXene in the artificial freshwater

containing *Daphnia* was measured at the same sampling time points as the *Daphnia* samples. The potential for Ti_3C_2 MXene deposition at a concentration of 5.0 mg L^{-1} in the absence of *Daphnia* was also examined by measuring the concentration of Ti_3C_2 MXene in the artificial freshwater at corresponding time points.

Text S6. CO_2 Generation Analysis

To ensure maximum degradation, 150 mg/L of Ti_3C_2 MXene was sealed and treated with 0.8 unit mL^{-1} of HRP and 300 μM of H_2O_2 in a PBS solution (pH = 6) for over 12 hours. Before initiating the reaction, a glass container holding 1 mL of 1 mol/L NaOH was suspended 2 cm above the liquid level in a closed apparatus to absorb any carbon dioxide (CO_2) produced during the reaction. In the control group, H_2O_2 was insteaded by DI water, while all other conditions remained identical. Each reaction was repeated three times to ensure data reliability. After 12 hours, the glass container with NaOH was removed, a small amount of phenolphthalein solution was added, and then 50 mM HCl was added dropwise until the solution became colorless. Subsequently, a small amount of methyl orange solution was added, and HCl was added dropwise while recording the volume of HCl used. Finally, the amount of CO_2 was calculated based on the HCl consumption.[16, 17]

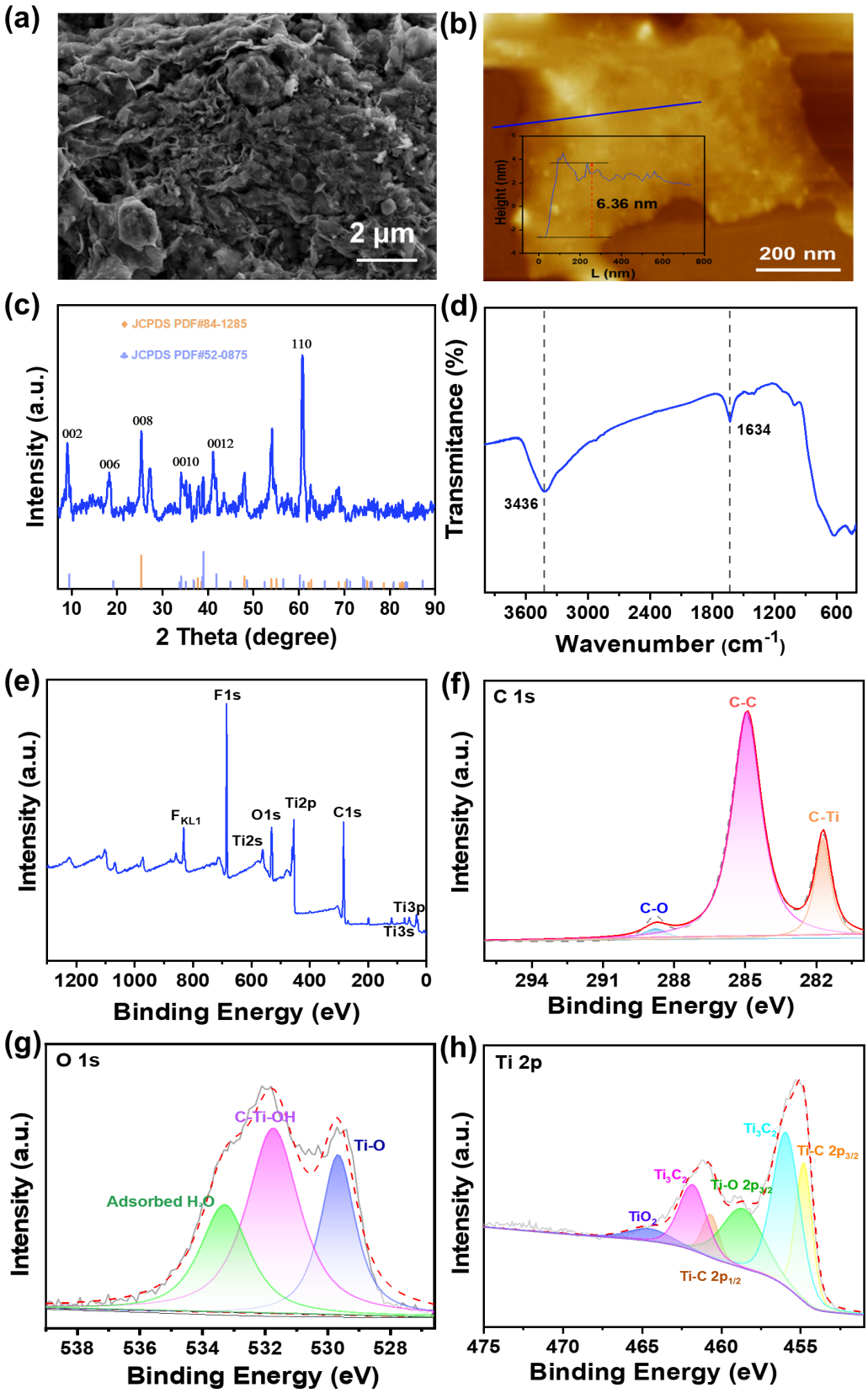

Fig. S1. Characterization of Ti_3C_2 MXene. (a) SEM (b) AFM images, (c) XRD pattern, (d) FT-IR spectra, (e) XPS survey spectra, and (f) C 1s, (g) O 1s, (h) Ti 2p peaks of Ti_3C_2 MXene.

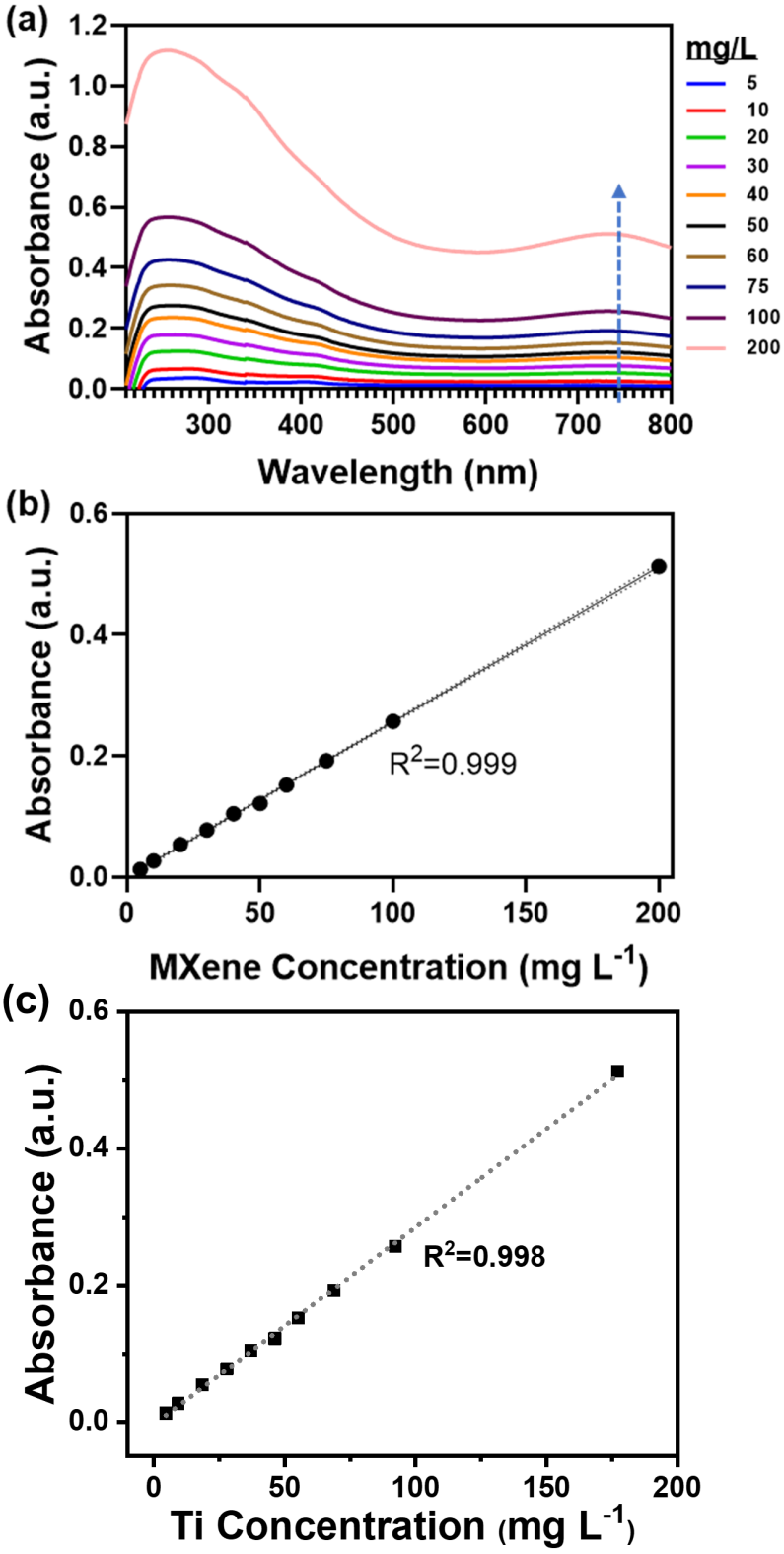

Fig. S2. (a) UV-vis absorption spectra of Ti_3C_2 MXene under concentration ranging from 5.0 to 200.0 mg L^{-1}, and (b) linear correlation between Ti_3C_2 MXene concentration and absorbance at 733 nm. (c) Linear regression curves of absorbance and titanium ion concentration, using AAS to test titanium ions, titanium recoveries in Ti_3C_2 MXene were ranged from 103.4 to 108.9.

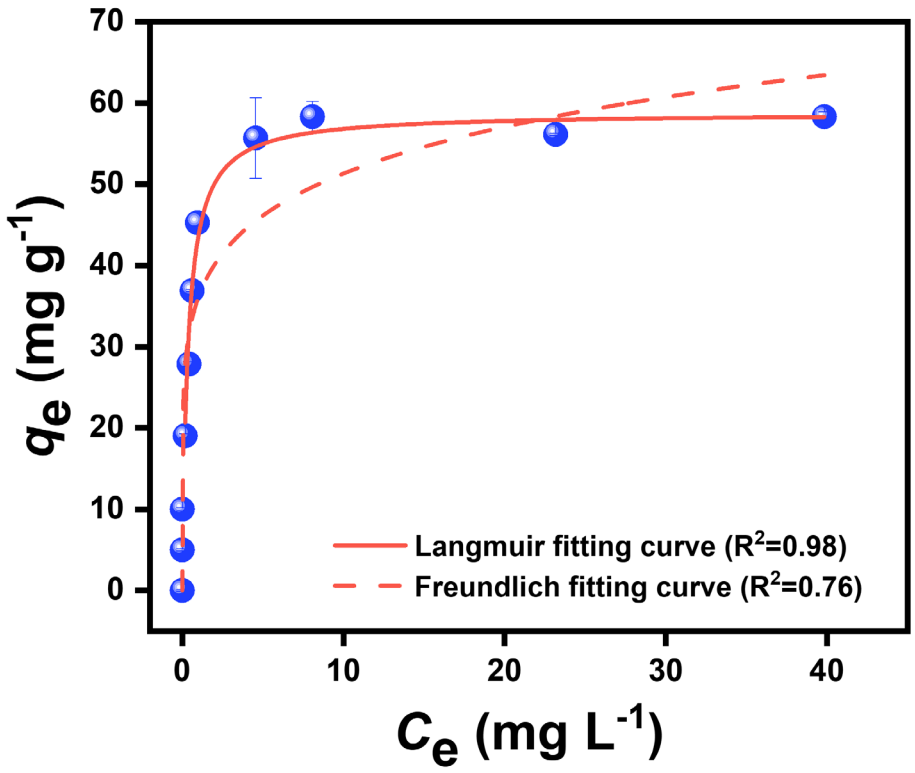

Fig. S3. Adsorption isotherms for HRP adsorption on Ti_3C_2 MXene (C_{Ti3C2} = 0.2 mg mL^{-1}, PBS buffer, pH = 7.0, 4 h incubation, 25 °C).

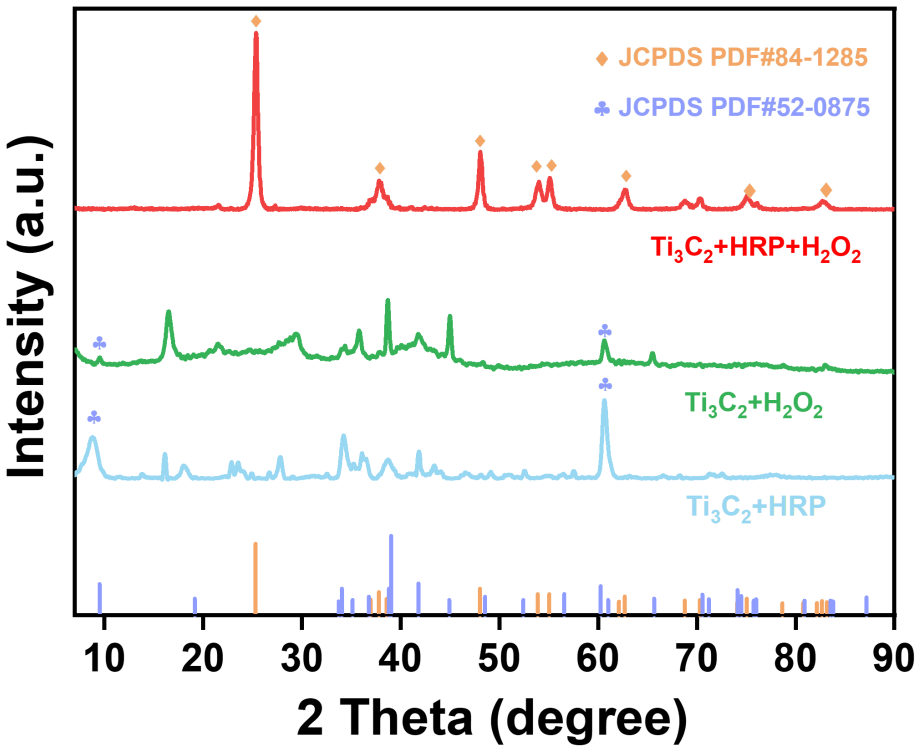

Fig. S4. The XRD patterns of Ti_3C_2 layers after various treatments provided insights into their structural transformations.

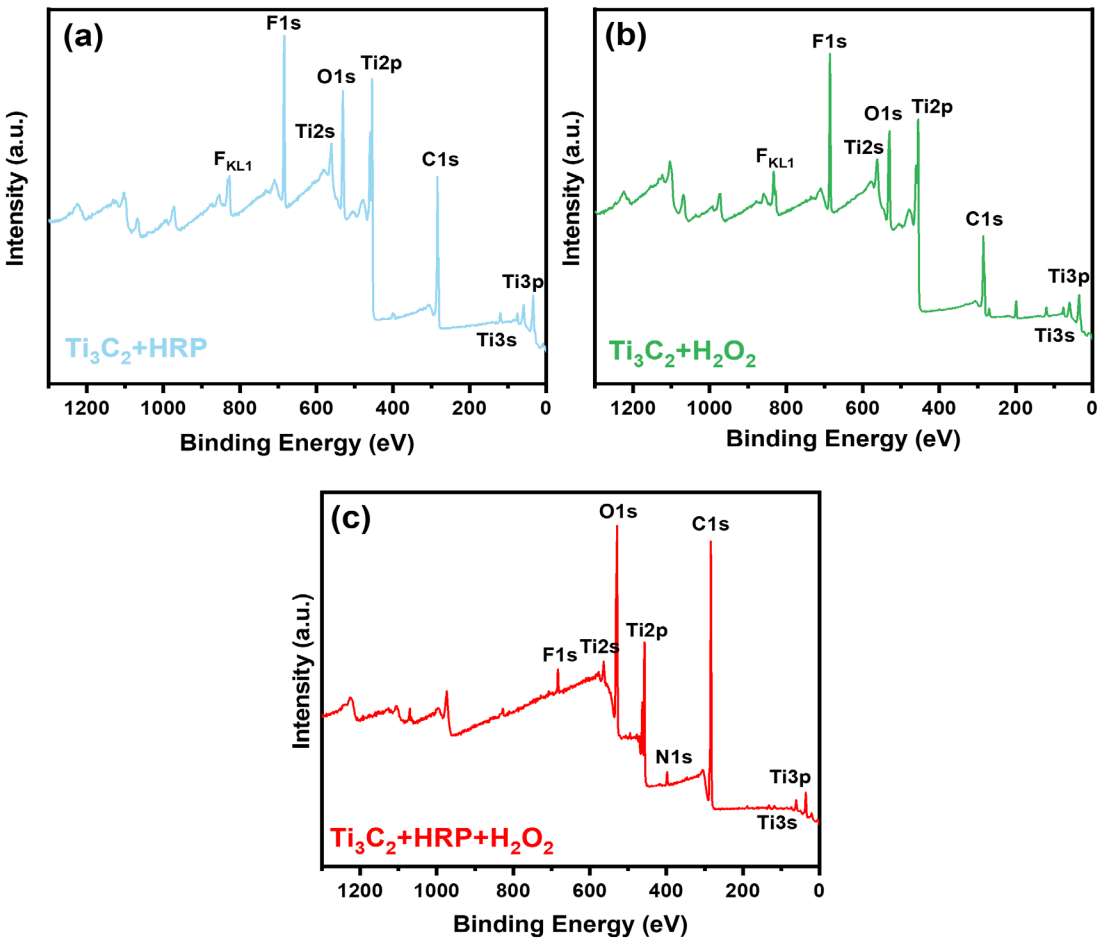

Fig. S5. The XPS survey spectra of Ti_3C_2 layers after various treatments revealed changes in elemental composition and bonding.

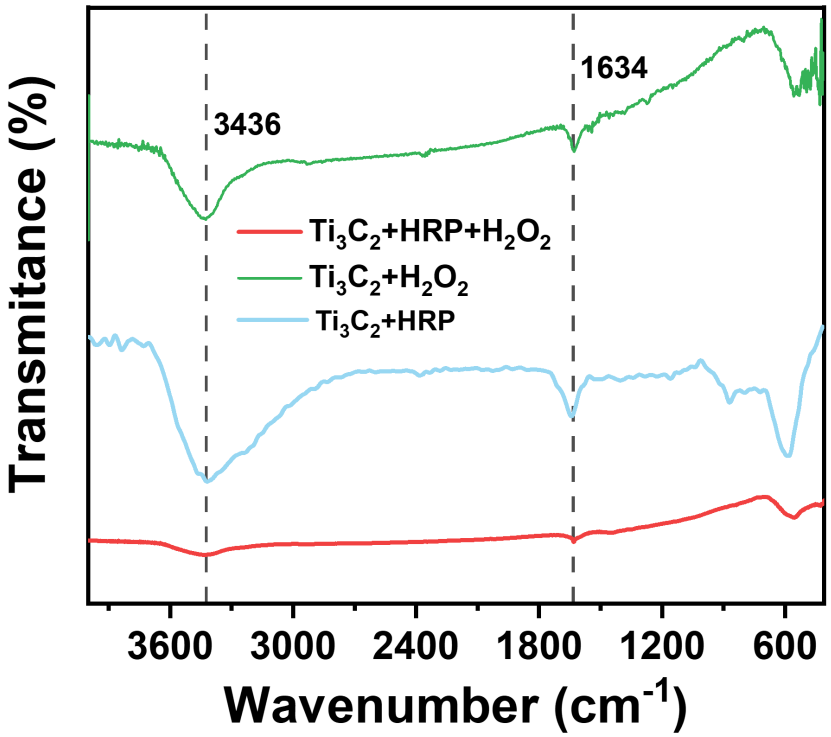

Fig. S6. The FT-IR spectra of Ti_3C_2 layers after various treatments provide insight into the surface functional groups and chemical changes occurring on the Ti_3C_2 surface.

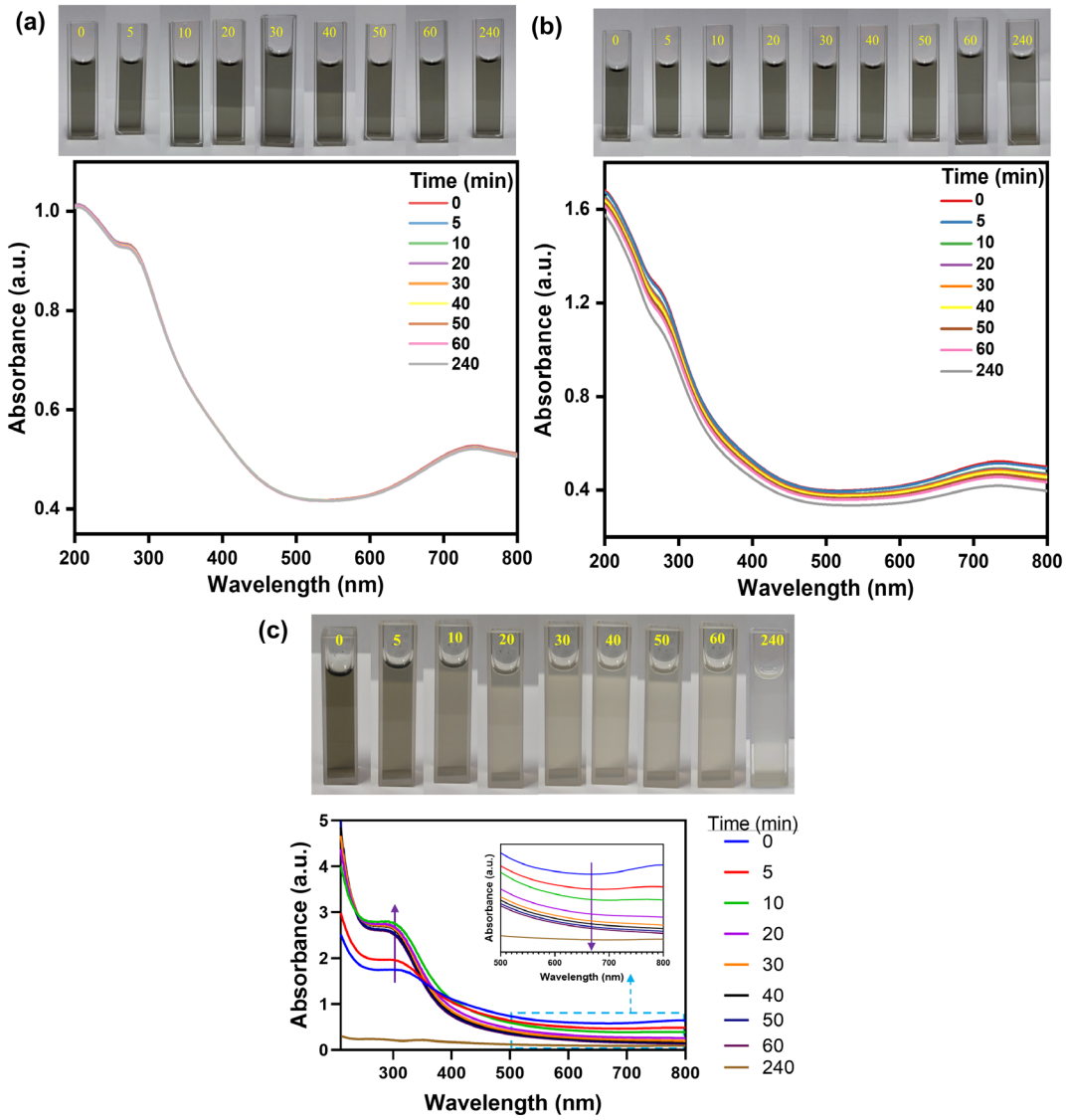

Fig. S7. Biodegradation of Ti_3C_2 MXene and changes in visually color and UV-vis absorption spectra of Ti_3C_2 MXene with only 0.80 unit mL^{-1} of HRP (a), with only 300 μM of H_2O_2 (b), and (c) with both HRP and H_2O_2. Reaction conditions: 50 mg L^{-1} of Ti_3C_2 MXene, pH = 6.0, 25 ° C.

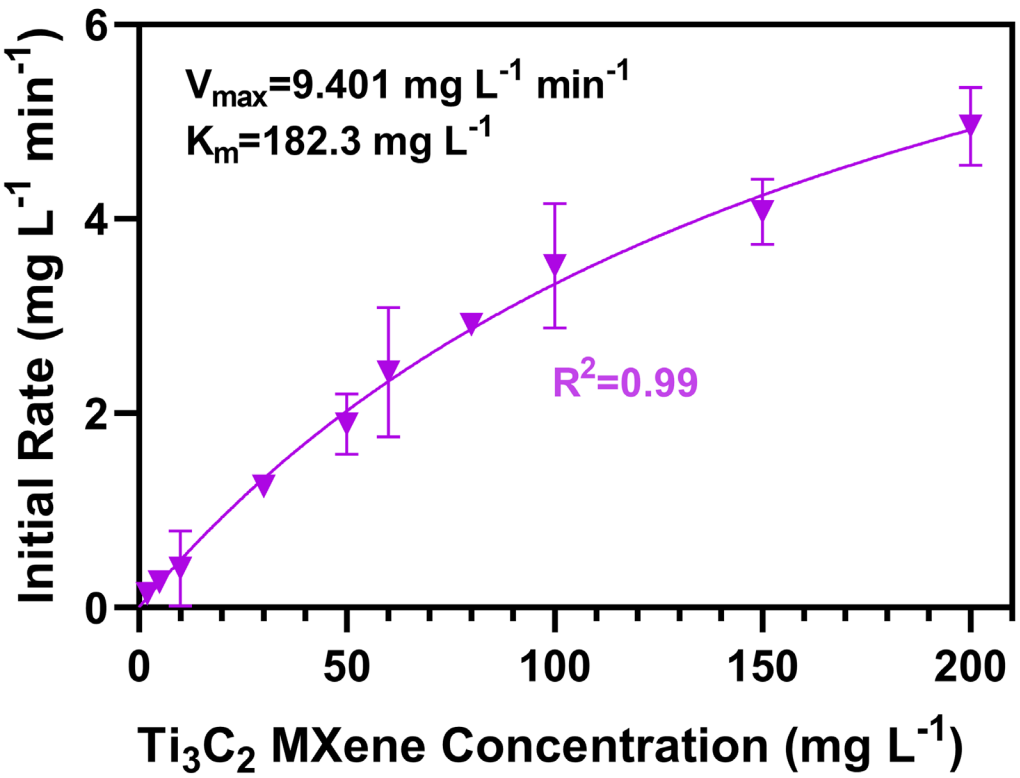

Fig. S8. The Michaelis–Menten kinetics of Ti_3C_2 MXene nanosheets. Reaction conditions: [Ti_3C_2 MXene] =2-200 mg L^{-1}, [HRP] = 0.8 unit mL^{-1}, pH = 6.0, 25 °C.

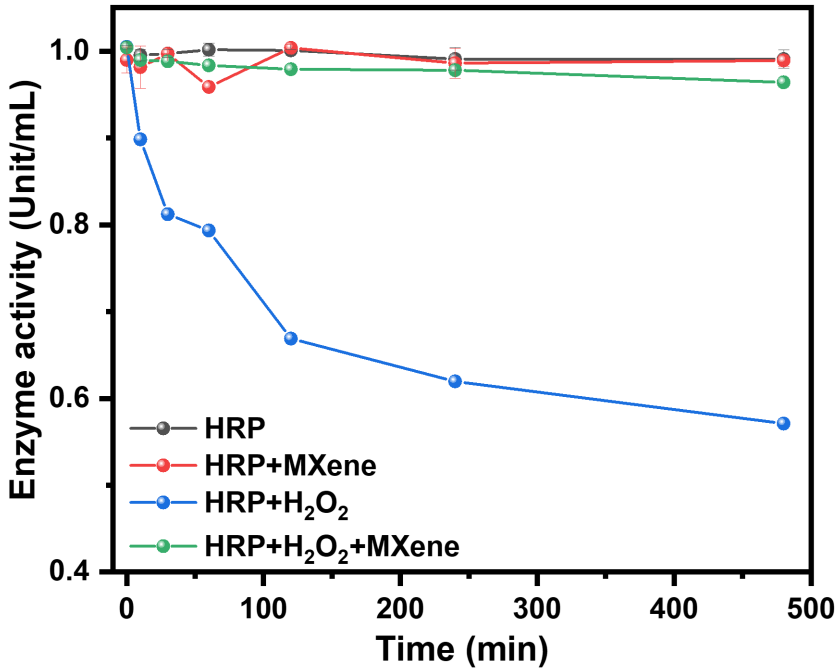

Fig. S9. Effect of different substances on HRP activity at different mixing times.

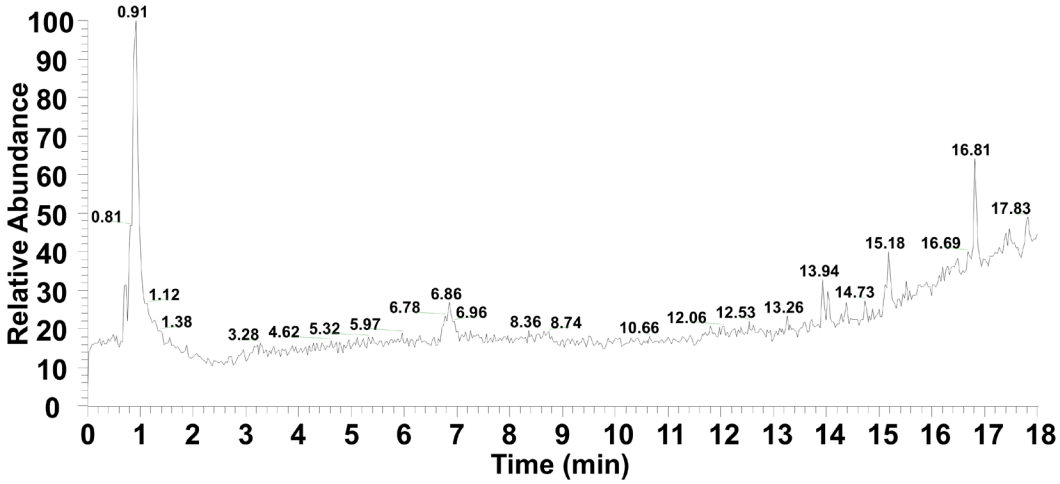

Fig. S10. HPLC-MS chromatogram of Ti_3C_2 MXene after HRP degradation.

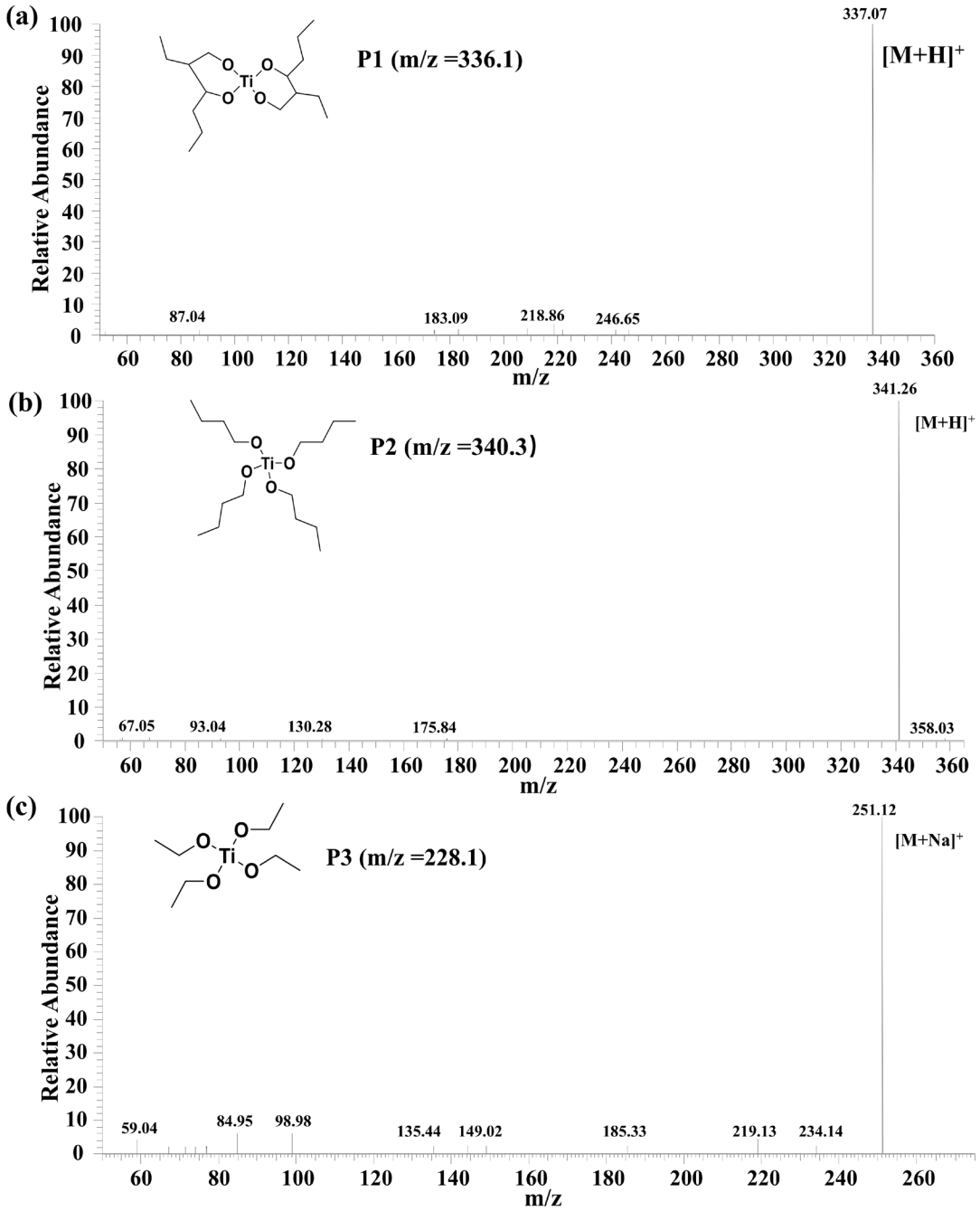
(a)
P1 (m/z =336.1)
337.07
[M+H]+
87.04
183.09
218.86
246.65
Relative Abundance
m/z
(b)
P2 (m/z =340.3)
341.26
[M+H]+
67.05
93.04
130.28
175.84
358.03
Relative Abundance
m/z
(c)
P3 (m/z =228.1)
251.12
[M+Na]+
59.04
84.95
98.98
135.44
149.02
185.33
219.13
234.14
Relative Abundance
m/z

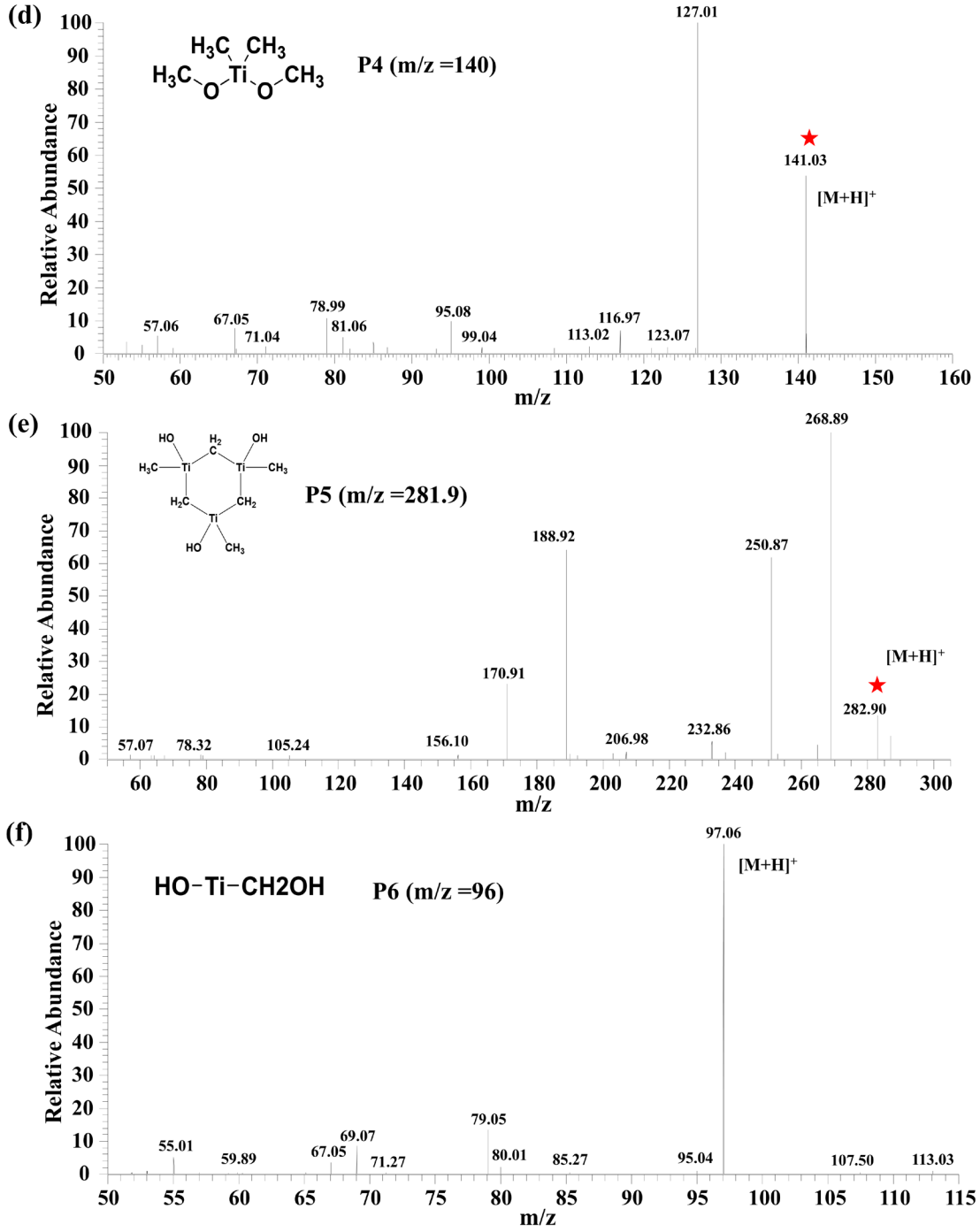

Fig. S11. The MS/MS spectra and the proposed structures of the possible degradation products of Ti_3C_2 MXene.

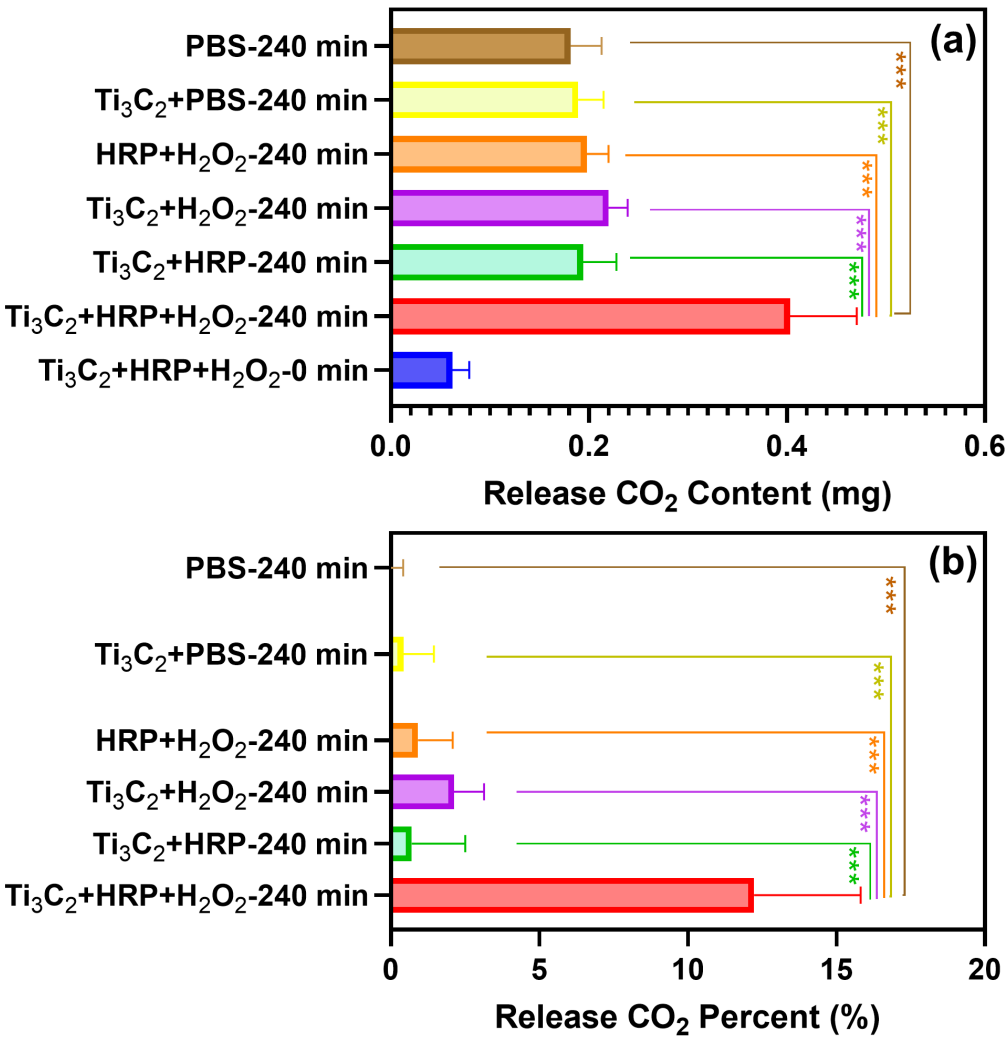

Fig. S12. The amount (a) and the percentage (b) of carbon dioxide released from Ti_3C_2 MXene reaction solutions under different conditions. Differences were statistically analyzed by one-way analysis of variance (ANOVA) followed by the LSD test for multiple comparisons ($p < 0.05$*, <0.01**, < 0.001***, n = 3) using SPSS 18.0 (IBM Company).

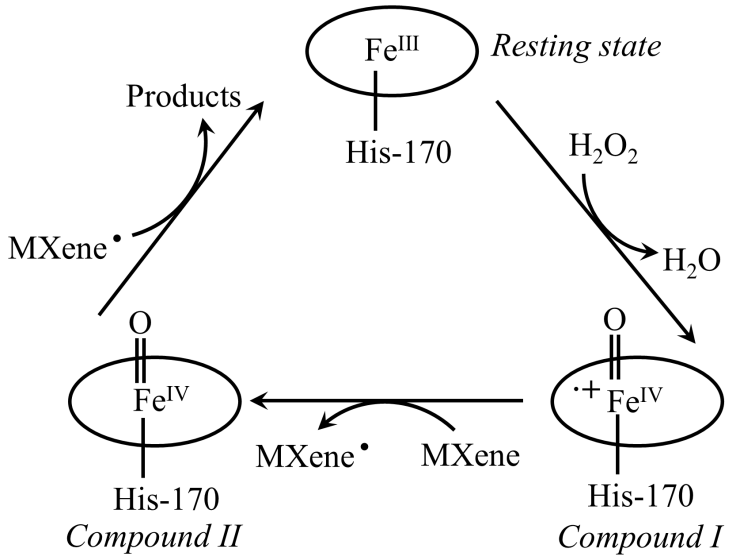

Fig. S13. Catalytic cycling mechanism of horseradish peroxidase in the presence of H_2O_2.

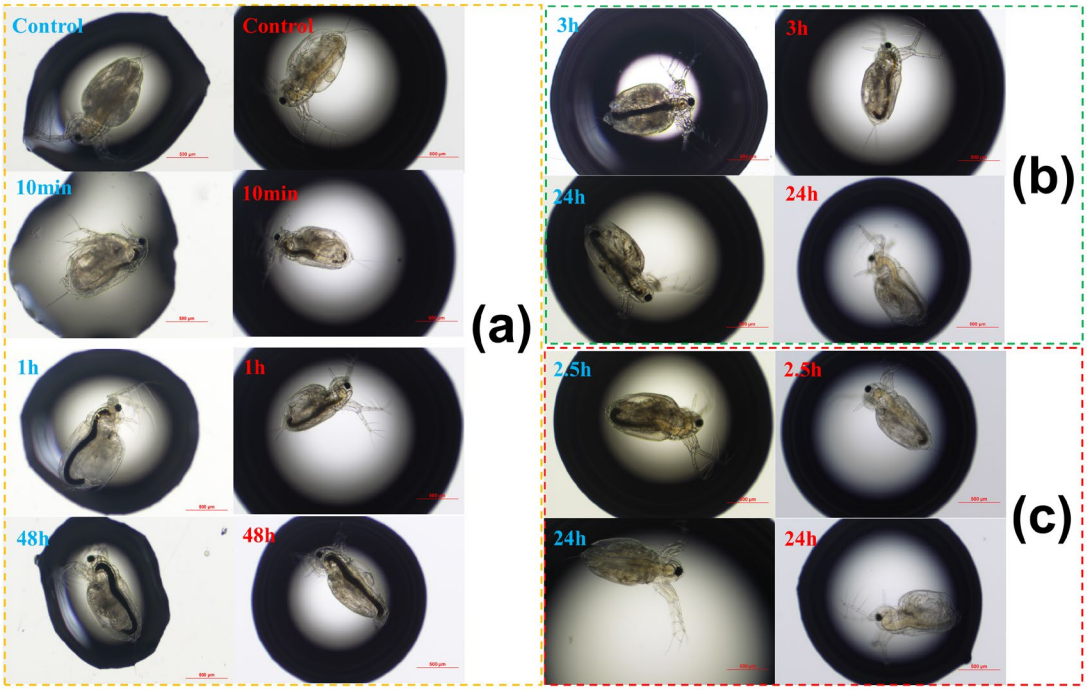

Fig. S14. Light microscope pictures of accumulation (a), depuration in DI water (b), and depuration with food (c) of Ti_3C_2 MXene before and after biodegradation by *D. magna* neonate. *Daphnia* were exposed to graphene in AF with a Ti_3C_2 MXene concentration of 5 mg/L Ti. Depuration occurred in the AL. Scale bar is 500 μm in the figures.

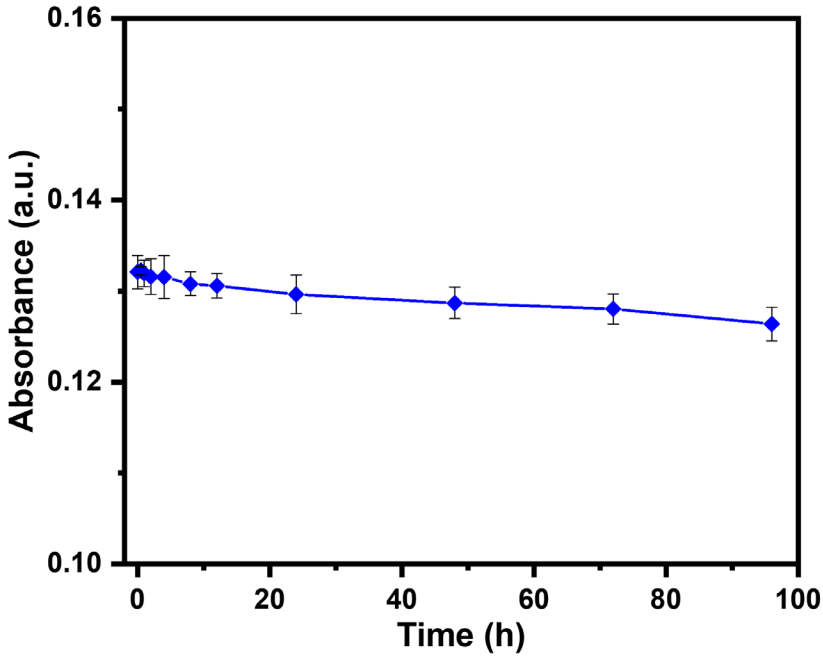

Fig. S15. The UV-vis absorbance data of Ti_3C_2 MXene in the tested exposure solutions.

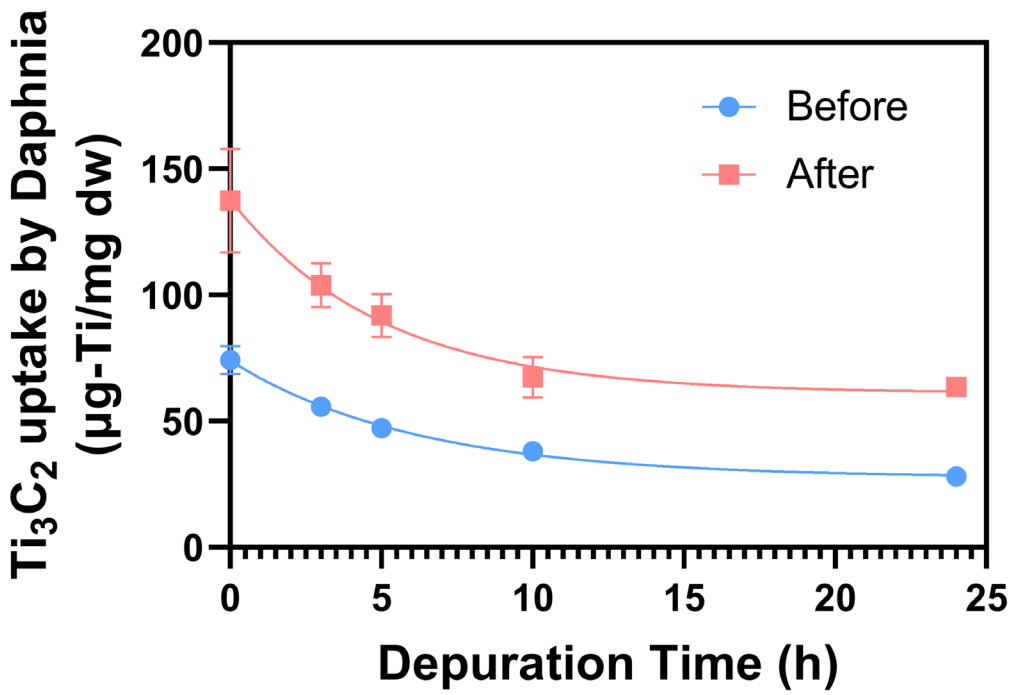

Fig. S16. Deputation kinetics of Ti_3C_2 MXene and the products in *Daphnia*.

Table S1. Simulated accumulation and deputation kinetic parameters of Ti_3C_2 MXene before and after biodegradation in *Daphnia*.

	maximum body burden (mg/g of dry weight)	BCF×10^4	depuration rate constant,k (h^{-1})	half-life, $t_{1/2}$ (h)	R^2 for first-Order depuration
Before	74.30±5.49	1.61	0.1627	4.26	0.9974
After	137.36±20.57	5.49	0.1997	3.47	0.9926

References

1. Lipatov, A.; Alhabeb, M.; Lukatskaya, M. R.; Boson, A.; Gogotsi, Y.; Sinitskii, A., Effect of Synthesis on Quality, Electronic Properties and Environmental Stability of Individual Monolayer Ti_3C_2 MXene Flakes. *Adv. Electron. Mater.* **2016,** *2*, (12), 1600255.
2. El Ghazaly, A.; Ahmed, H.; Rezk, A. R.; Halim, J.; Persson, P.; Yeo, L. Y.; Rosen, J., Ultrafast, One-Step, Salt-Solution-Based Acoustic Synthesis of Ti_3C_2 MXene. *Acs Nano* **2021,** *15*, (3), 4287-4293.
3. Alhabeb, M.; Maleski, K.; Mathis, T. S.; Sarycheva, A.; Hatter, C. B.; Uzun, S.; Levitt, A.; Gogotsi, Y., Selective Etching of Silicon from Ti_3SiC_2 (MAX) To Obtain 2D Titanium Carbide (MXene). *Angew. Chem.-Int. Edit.* **2018,** *57*, (19), 5444-5448.
4. Li, X. J.; Zeng, C. M.; Fan, G. Y., Magnetic RuCo Nanoparticles Supported on Two-Dimensional Titanium Carbide as Highly Active Catalysts for the Hydrolysis of Ammonia Borane. *Int. J. Hydrog. Energy* **2015,** *40*, (30), 9217-9224.
5. Peng, Q. M.; Guo, J. X.; Zhang, Q. R.; Xiang, J. Y.; Liu, B. Z.; Zhou, A. G.; Liu, R. P.; Tian, Y. J., Unique Lead Adsorption Behavior of Activated Hydroxyl Group in Two-Dimensional Titanium Carbide. *J. Am. Chem. Soc.* **2014,** *136*, (11), 4113-4116.
6. Foratirad, H.; Baharvandi, H. R.; Maragheh, M. G., Chemo-Rheological Behavior of Aqueous Titanium Carbide Suspension and Evaluation of the Gelcasted Green Body Properties. *Mater. Res.-Ibero-am. J. Mater.* **2017,** *20*, (1), 175-182.
7. Zhang, C. F. J.; Pinilla, S.; McEyoy, N.; Cullen, C. P.; Anasori, B.; Long, E.; Park, S. H.; Seral-Ascaso, A.; Shmeliov, A.; Krishnan, D.; Morant, C.; Liu, X. H.; Duesberg, G. S.; Gogotsi, Y.; Nicolosi, V., Oxidation Stability of Colloidal Two-Dimensional Titanium Carbides (MXenes). *Chem. Mat.* **2017,** *29*, (11), 4848-4856.
8. Xia, F. J.; Lao, J. C.; Yu, R. H.; Sang, X. H.; Luo, J. Y.; Li, Y.; Wu, J. S., Ambient Oxidation of Ti_3C_2 MXene Initialized by Atomic Defects. *Nanoscale* **2019,** *11*, (48), 23330-23337.
9. Feng, Y. P.; Colosi, L. M.; Gao, S. X.; Huang, Q. G.; Mao, L., Transformation and Removal of Tetrabromobisphenol A from Water in the Presence of Natural Organic Matter via Laccase-Catalyzed Reactions: Reaction Rates, Products, and Pathways. *Environ. Sci. Technol.* **2013,** *47*, (2), 1001-1008.
10. Feng, Y. P.; Lu, K.; Gao, S. X.; Mao, L., The Fate and Transformation of Tetrabromobisphenol A in Natural Waters, Mediated by Oxidoreductase Enzymes. *Environ. Sci.-Process Impacts* **2017,** *19*, (4), 596-604.
11. Feng, Y. P.; Shen, M. Y.; Wang, Z.; Liu, G. G., Transformation of Atenolol by a Laccase-Mediator System: Efficiencies, Effect of Water Constituents, and Transformation Pathways. *Ecotox. Environ. Safe.* **2019,** *183*, 109555.
12. Feng, Y. P.; Lu, K.; Mao, L.; Guo, X. K.; Gao, S. X.; Petersen, E. J., Degradation of ^{14}C-Labeled Few Layer Graphene via Fenton Reaction: Reaction Rates, Characterization of Reaction Products, and Potential Ecological Effects. *Water Res.* **2015,** *84*, 49-57.
13. Guo, X. K.; Dong, S. P.; Petersen, E. J.; Gao, S. X.; Huang, Q. G.; Mao, L., Biological Uptake and Depuration of Radio-labeled Graphene by *Daphnia magna*. *Environ. Sci. Technol.* **2013,** *47*, (21), 12524-12531.
14. Fadare, O. O.; Wan, B.; Guo, L. H.; Xin, Y.; Qin, W. P.; Yang, Y., Humic Acid Alleviates the Toxicity of Polystyrene Nanoplastic Particles to *Daphnia magna*. *Environ. Sci.-Nano* **2019,** *6*, (5), 1466-1477.
15. Wu, J. Y.; Ye, W. B.; Feng, Y. P.; Lao, W. H.; Li, J. C.; Lu, H. J.; Liu, G. G.; Su, G. Y.; Deng, Y. R., Aquatic Photolysis of High-Risk Fluorinated Liquid Crystal Monomers: Kinetics, Toxicity Evaluation, and Mechanisms. *Water Res.* **2024,** *255*, 121510.
16. Peng, Z.; Liu, X. J.; Zhang, W.; Zeng, Z. T.; Liu, Z. F.; Zhang, C.; Liu, Y.; Shao, B. B.; Liang, Q. H.; Tang, W. W.; Yuan, X. Z., Advances in the Application, Toxicity and

Degradation of Carbon Nanomaterials in Environment: A Review. *Environ. Int.* **2020,** *134*, 105298.
17. Zumstein, M. T.; Schintlmeister, A.; Nelson, T. F.; Baumgartner, R.; Woebken, D.; Wagner, M.; Kohler, H. P. E.; McNeill, K.; Sander, M., Biodegradation of Synthetic Polymers in Soils: Tracking Carbon into CO_2 and Microbial Biomass. *Sci. Adv.* **2018,** *4*, (7), eaas9024.